A Mathematical Model of Road Pavement Strength Considering Thermophysical Property Variations

Assel Yesbolat
L.B. Goncharov Kazakh Automobile and Road Institute, Almaty, Kazakhstan
ashkeeva@mail.ru

Saniya Kiyalbay
L.B. Goncharov Kazakh Automobile and Road Institute, Almaty, Kazakhstan
sanina8@mail.ru

Dauren Yessentay
L.B. Goncharov Kazakh Automobile and Road Institute, Almaty, Kazakhstan
yessentaydauren063@gmail.com (corresponding author)

Received: 27 January 2026 | Revised: 19 March 2026 | Accepted: 1 April 2026

Licensed under a CC-BY 4.0 license | Copyright (c) by the authors | *DOI: https://doi.org/10.48084/etasr.17798*

ABSTRACT

Asphalt concrete pavements are highly sensitive to variations in temperature, moisture, and material density. These variations significantly affect the pavements' mechanical performance during service. This study presents a theoretical model that assesses how thermophysical factors influence the reduction of asphalt concrete's compressive strength. The model uses a gradient-search approach to evaluate strength behavior under combined changes in density, moisture content, and temperature during heating and freezing. The input parameters were obtained from laboratory experiments carried out under controlled conditions. Asphalt concrete specimens were tested within a temperature range of −20 °C to 60 °C. During the experiments, the density of the specimens ranged from a maximum practical value of 0.99 t/m³ to a critical value of 0.87 t/m³, which is associated with structural degradation; the moisture content was maintained within defined limits. The proposed methodology determines the minimum compressive strength resulting from the combined influence of the studied factors. These results can be used to evaluate the performance and durability of asphalt concrete pavements under different environmental conditions.

Keywords-asphalt concrete; strength; thermophysical factors; temperature; gradient-based modeling

I. INTRODUCTION

In regions with a sharply continental climate, road pavements frequently deteriorate intensely during the winter–spring period. One of the primary causes of this deterioration is the rapid thawing of the frozen subgrade [1], which significantly reduces the pavement structure's bearing capacity [2]. Similar damage mechanisms occur when technological deficiencies arise during construction, particularly when pavement layers are insufficiently compacted [3]. Analyzing road performance under operational conditions reveals three key factors that predominantly influence pavement degradation: initial compaction density of pavement layers in the early stages of operation (X_1), pavement structure moisture content (X_2), and daily air temperature fluctuations that characterize the pavement surface's cooling and heating cycles (X_3) [4]. Under dynamic traffic loads, these factors cause substantial variations in the mechanical properties of pavement materials. This leads to the development of various deformation modes and structural failures on the pavement surface. Practical experience in ensuring the strength and durability of asphalt concrete pavements indicates that a compaction coefficient of at least K = 0.99 is necessary [5]. Reduced compaction levels indicate insufficient strength of the pavement layer, which is primarily determined by the characteristics of the mineral aggregate skeleton and the proportions of the mixture components [6]. Additionally, moisture accumulation within the pore structure of asphalt concrete during its service life may further degrade its mechanical properties [7]. Thermal effects induced by solar radiation significantly contribute to the deterioration of asphalt concrete pavements. Exposure to solar radiation causes intensive heating of the asphalt concrete layer, reducing its resistance to deformation [8]. The bituminous binder absorbs a considerable amount of thermal energy due to its relatively high heat capacity compared to the mineral aggregate

component. Asphalt concrete mixtures typically contain fine aggregates, including mineral filler ranging from 9 to 12%, which fills pore spaces and increases the thermal conductivity of the mineral skeleton. Therefore, pavement surface temperatures may reach 60–65 °C under intense solar radiation. Under such thermal conditions and in the presence of dynamic traffic loads, asphalt concrete becomes highly susceptible to shear deformation as internal shear stresses within the material increase significantly. Environmental factors impact road structures, inducing complex, interrelated heat and moisture transfer processes within the subgrade and pavement layers [9]. Temperature variations promote moisture migration, and moisture accumulation and phase transformations enhance heat transfer processes [10]. Therefore, heat and moisture exchange phenomena in pavement systems must be considered together rather than separately. Soil and pavement layers have been shown to be air-permeable materials with interconnected pore networks. This structural characteristic creates favorable conditions for heat and mass transfer processes, including air and vapor exchange, within the subgrade and pavement layers. These processes occur as long as the soil's moisture content does not reach its full water-holding capacity. At full saturation, pore spaces are filled with liquid water, resulting in the cessation of air and vapor exchange. These mechanisms play a crucial role in the evolution of the thermal-moisture regime of road structures and directly affect their mechanical performance. Authors in [11, 12] demonstrated that higher temperatures reduce stiffness and shear resistance, making the material more susceptible to rutting and permanent deformation. Authors in [13] focused on moisture-related damage, showing that moisture penetration accelerates strength degradation, particularly under cyclic loading and freeze–thaw conditions. Moisture damage is commonly associated with the loss of adhesion between bitumen and mineral aggregates, as well as the development of pore pressure during loading. Despite the existing studies on the durability of asphalt concrete, most approaches only consider the effects of temperature, moisture, and density individually, without considering their combined nonlinear interactions. This limitation hinders the ability to predict strength degradation reliably under realistic operating conditions, especially in regions with sharply continental climates, which are characterized by large seasonal temperature variations (from −20 °C to +70 °C) and pronounced freeze–thaw cycles. The main research problem addressed in the current study is the lack of an integrated model capable of describing the combined influence of these parameters. In order to address this issue, this study presents and validates an experimental, gradient-based mathematical model that quantifies the compressive strength of asphalt concrete as a function of density (X_1), moisture content (X_2), and temperature (X_3). The novelty of this work lies in: constructing a polynomial response function, F(X_1, X_2, X_3), based on a full factorial experimental design that captures first-order main effects and pairwise interaction terms, applying a gradient-based optimization algorithm to identify the minimum compressive strength under combined factor variation, and providing a quantitative decomposition of the relative contribution of each factor—namely, density, moisture, and temperature—to the total strength variability within the investigated operating range. The proposed approach produces an analytical expression suitable for iterative optimization and can be calibrated for other asphalt mixture types.

II. MATERIALS AND METHOD

A. Theoretical Foundations of the Gradient Method

Gradient methods are a type of first-order method. The gradient of a function, F(X), is a vector whose components are the function's partial derivatives with respect to each variable. At each point X, the gradient is directed toward the point of maximum increase of the function and is perpendicular to the level line (surface of constant value) of the function. In the iterative process, the gradient of the function at point $X(k)$ is chosen as the direction of movement to the next point. Denoting the gradient of F(X) at $X(k)$ by ∇F($X(k)$) and setting R = ∇F($X(k)$), the search for the maximum is [14]:

$$X^{(k+1)} = X^{(k)} + h_k \cdot p_k \quad (1)$$

$$X^{(k+1)} = X^{(k)} + h_k \cdot \nabla F\,(X^{(k)}) \quad (2)$$

where $p_k$is a vector specifying the direction of movement from the current point $X^{(k)}$to the next point $X^{(k+1)}$of the iterative sequence, and $h_k$is a positive scalar determining the step size along the direction p_k. The quantity h_k is referred to as the step size or simply the step. In the equation, the sign "+" corresponds to searching for a maximum, while the sign "-" corresponds to searching for a minimum of the function. The vector ratio corresponds to n ratios shown in coordinate form:

$$X_j^{(kn)} = X_j^{(k)} \pm h_k \cdot \partial F(X^{(k)})/dX_j \quad (3)$$

where $X_j^{(kn)}$is the trial value of the variable $X_j$at iteration k, obtained by perturbing the current point $X^{(k)}$ by $\pm h_k$along the j-th coordinate direction. This notation is used to identify the trial points used for the numerical estimation of gradient components, while $X^{(k)}$ denotes the iterative points of the optimization process.

B. Criteria for Method Modification

In the present study, the step size, h_k, was determined using a bisection strategy. The initial step size was set to $h_0 = 0.5$ (in coded units). At each iteration, if the response function value, $F(X^{(k+1)})$, did not decrease relative to $F(X^{(k)})$, the step size was reduced according to the rule, $h_{(k+1)}=h_k/2$. Otherwise, the step size remained unchanged. The iterative process terminated when the gradient magnitude, $|\nabla F(X^{(k)})|$, became smaller than the prescribed tolerance, $\varepsilon = 0.01$, or when the function value reached its minimum within the feasible region of the experimental design. The iterative process stops when it approaches the desired extreme point. The termination criteria, indicating that the last point of the sequence $X^{(k)}$ is sufficiently close to the extreme point X^x, are the gradient modulus, the modulus of the difference between the optimized function at two adjacent points of the sequence, or both:

$$[\nabla F(X^k)] = \sqrt{\sum_{j=1}^{n}\left(\frac{dF\,(X^{(k)})}{dX_j}\right)} \quad (4)$$

$$\left[F\left(X^{(k+1)}\right) - F(X^{(k)})\right] \quad (5)$$

The values of the criteria are compared with sufficiently small positive numbers, E_g and E_x, which correspond to the required accuracy of the solution. The iterative process terminates when the inequality is fulfilled:

$$\left[F\left(X^{(k+1)}\right) < E_g\right] \quad (6)$$

$$\left[F\left(X^{(k+1)}\right) - F(X^{(k)})\right] < E_x \quad (7)$$

Practical application of gradient methods requires determining the partial derivatives of the objective function, $F(X)$, with respect to each variable, X_j, at every step. This can be done using analytical or numerical methods. The latter are more commonly used for sufficiently complex functions in routine calculations. Numerical methods are divided into unilateral and bilateral finite difference methods [6, 8]. In the first case, the partial derivatives at point $X^{(k)}$ are found using:

$$\frac{dF\,(X^{(k)})}{dX_j} = \frac{F\,(X^{(k)}+\Delta X_j)-F(X^{(k)})}{\Delta X_j} \quad (8)$$

$$\frac{dF\,(X^{(k)})}{dX_j} = \frac{F\,(X^{(k)})-F(X^{(k)}+\Delta X_j)}{\Delta X_j} \quad (9)$$

where ΔX_j is the increment (trial step) of variable Xj. In the method of bilateral finite differences, the net derivative is:

$$\frac{dF\,(X^{(k)})}{dX_j} = \frac{F\,(X^{(k)}+\Delta X_j)-F(X^{(k)}-\Delta X_j)}{2\cdot\Delta X_j} \quad (10)$$

C. Experimental Determination of Model Parameters

Laboratory experiments were conducted under controlled conditions to obtain the input parameters necessary for the mathematical model. Compression tests were performed on fine-grained asphalt concrete specimens using a hydraulic testing press. During these tests, the corresponding response parameter, F_i, was determined based on the recorded compressive forces. The physical and mechanical parameters (X_1, X_2, X_3) used in the model were determined experimentally. Lower (-) and upper (+) boundary values were specified for each parameter and used to form the experimental design. At the lower limit, all reagents were practically similar, with their tangential stresses ranging from 0.347 MPa to 0.557 MPa. Compressive strength under uniaxial loading was selected as the primary response parameter because it can be directly measured under controlled laboratory conditions (hydraulic press, cylindrical specimens Ø70 mm × 70 mm) and ensures high reproducibility across the investigated temperature and moisture regimes. Within the temperature range of −20 °C to +70 °C, compressive strength exhibits a monotonic, physically interpretable response to the three studied factors, making it a suitable objective function for gradient-based optimization. Additionally, variations in compressive strength reflect the reduction in load-bearing capacity preceding visible pavement distress, such as rutting, shoving, and cracking, during the spring–autumn transition periods typical of continental climates. These periods represent the main service conditions considered in this study, with the testing procedure presented in Figure 1. Cylindrical specimens of fine-grained asphalt concrete were prepared under laboratory conditions before testing. The density of the specimens under compression (X_1) ranged from 0.87 t/m³ to 0.99 t/m³. The specimens were conditioned for up to 36 h under controlled temperature regimes before testing. The upper temperature level (+70° C) was achieved using a laboratory drying oven, while the lower temperature level (-20° C) was achieved using a freezer. These temperature levels correspond to the upper and lower values specified in Table I.

Fig. 1. Testing of asphalt concrete samples.

TABLE I. PLANNING ON EXPERIMENTAL DATA

j/I	X_0	X_1	X_2	X_3	X_1X_2	X_1X_3	X_2X_3	$X_1X_2X_3$	**Experimental indicators F_1, MPA**
1	+	-	-	-	+	+	+	-	10.54
2	+	-	-	+	+	-	-	+	12.85
3	+	-	+	-	-	+	-	+	14.96
4	+	+	-	-	-	-	+	+	16.53
5	+	+	-	+	-	+	-	-	17.52
6	+	-	+	+	-	-	+	-	17.93
7	+	+	+	-	+	-	-	-	18.59
8	+	+	+	+	+	+	+	+	19.28
B_i	16.02	1.95	1.66	0.87	-0.71	-0.44	-0.05	-0.12	

Fine-grained asphalt concrete with a maximum thermal conductivity of 1.78 W/(m·K) was used for the laboratory tests. The moisture content of the specimens (X_2) was adjusted by conditioning them in a water bath for 48 h, while the temperature of the asphalt concrete specimens (X_3) was controlled using a drying oven and a freezer. The sample temperature limits simulated actual temperature fluctuations of the asphalt concrete sample due to air temperature in summer or winter. The full factorial experimental method was used to analyze the results. This method is based on the assumption that the continuous function F = $f(X_1, X_2, X_3)$, which has all derivatives at the given points X_{01}, X_{02}, X_{03}, can be expanded into a Taylor series [4]:

$$F = B_0 + B_1 X_1 + B_2 X_2 + B_3 X_3 + \cdots + B_{ij} X_{ij} \quad (11)$$

where P is the compressive strength of asphalt concrete, MPa; B is the value of the response function at the origin; and X_{01}, X_{02}, X_{03}, X_1, X_2, X_3 are the strength indicators of asphalt concrete. The Taylor series [6, 14] with three indicators is:

$$F\left(X_1, X_2, X_3\right) = B_0 + B_1 X_1 + B_2 X_2 + B_3 X_3 + B_{12} X_1 X_2 + B_{13} X_1 X_3 + B_{23} X_2 X_3 + B_{123} X_1 X_2 X_3 \quad (12)$$

$$B_{ij} = \sum_{i=1}^{n} F_{i/n} \quad (13)$$

where n is the number of experiments (n=8), and i is the serial number of each experiment [5]. The gradient optimization

method was used to determine the minimum of the response function F (X_1, X_2, X_3), given by:

$$|\nabla\tau(X_k)| = \sqrt{h \cdot \left(\frac{dF_0}{dX_1}\right)^2 + \left(\frac{dF_0}{dX_2}\right)^2 + \left(\frac{dF_0}{dX_3}\right)^2} \qquad (14)$$

The initial search point X_1, X_2, X_3 was taken as the central point of the factor space corresponding to the zero coded values of the variables. A gradient-based optimization approach was employed to determine the minimum of the three-variable response function F (X_1, X_2, X_3). The search procedure was initiated from the central point of the factor space corresponding to the zero-coded values of the variables. The optimization was carried out using a fixed step size that varied within the range of $h = 0$ to $h = 3.0$, in accordance with the experimental design. The components of the gradient vector were obtained by analytically differentiating (14) with respect to X_1, X_2, and X_3. At each iteration, the response function was evaluated using updated factor levels determined by the specified step size. This iterative process was repeated using the newly obtained values of X_1, X_2, and X_3 until the response function F (X_1, X_2, X_3) reached its minimum value. The response function value at the optimal point was calculated, with the determined model coefficients and factor levels. This value represents the predicted compressive strength of the asphalt concrete specimen corresponding to the optimal combination of studied factors.

III. RESULTS AND DISCUSSION

A. Calculation Scheme

Figure 2 shows a block diagram of the calculation algorithm, which was developed based on numerical optimization and response function evaluation. The diagram presents the logical structure of the computational approach used to analyze variations in the strength-related parameters of pavement materials. The calculation algorithm involves successively evaluating the response function, assessing gradient components, estimating the gradient magnitude, and iteratively updating factor levels until a limiting condition corresponding to an extreme response function value is achieved. The proposed mathematical model optimizes the strength characteristics of asphalt concrete pavement by considering asphalt concrete density (X_1), moisture content (X_2), and the heating or freezing temperature of pavement materials (X_3). The algorithm's structure highlights the combined influence of these factors on the predicted strength behavior of asphalt concrete. The results of the numerical calculation of asphalt concrete compressive strength considering variations in temperature and moisture content are summarized in Table II. Table II demonstrates the iterative factor values, the gradient components of the response function, the step-scaled gradients, and the corresponding gradient magnitudes, revealing the convergence behavior of the optimization process. The gradient magnitude, $|\nabla F(X^{(k)})|$, decreased from 3.34 at iteration 1 to 1.76 at iteration 2, and increased to 2.34 at iteration 3. As the algorithm approached the boundary of the feasible region, the gradient magnitude continued to increase. This behavior reflects the non-convex nature of the polynomial response surface and the presence of interaction effects between the governing factors. The change in gradient direction observed at iterations 4–6 indicates a transition in the search trajectory associated with coupled temperature-moisture effects in the viscoelastic asphalt concrete system. The results obtained are consistent with viscoelastic theory: at elevated temperatures (X_3 = ±70°C), the bituminous binder exhibits increased viscous behavior, resulting in reduced stiffness and compressive strength.

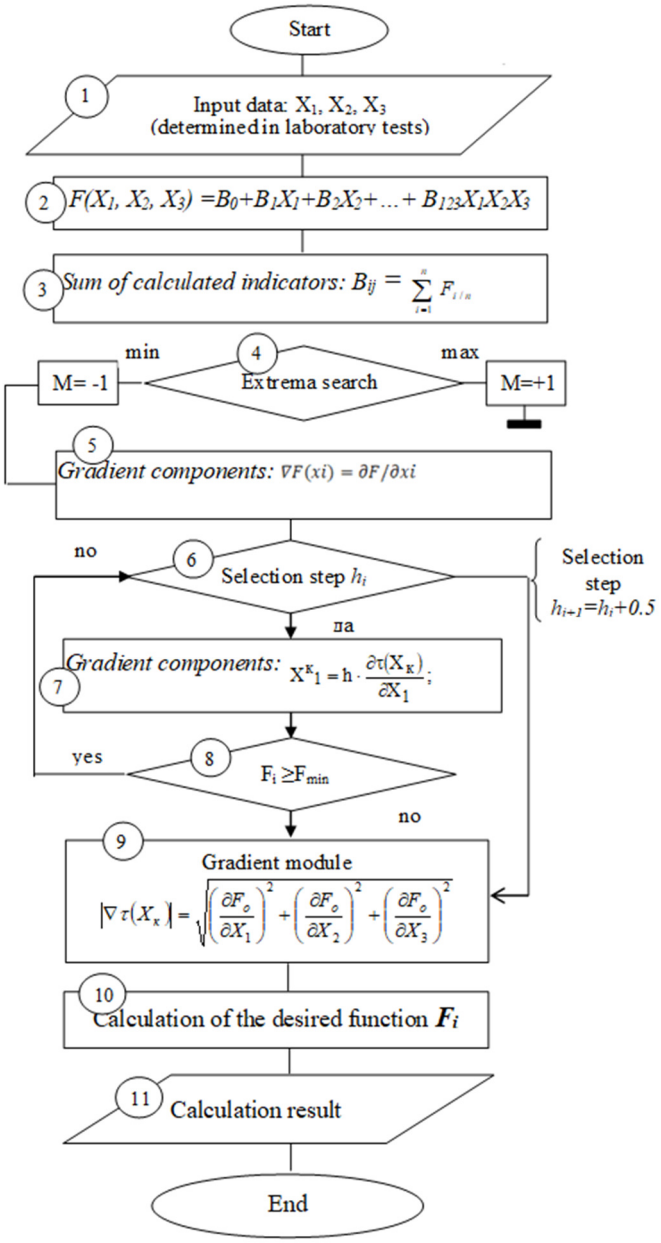

Fig. 2. Calculation algorithm.

The gradient method identified this region as corresponding to minimum strength conditions. The iterative process ended at the seventh iteration when the factor values reached the boundaries of the experimental design domain. This ensures that the obtained optimum remains within physically admissible conditions.

TABLE II. NUMERICAL RESULTS OF ASPHALT CONCRETE COMPRESSIVE STRENGTH CALCULATION

k	X^k (X_1^k/ X_2^k/ X_3^k)	dP/dX^k	$h \cdot dP/dX^k$	$\lvert\nabla F(X^k)\rvert$
1	-/-/-	0/0/0	3.08/2.50/1.18	3.34
2	0.77/0.62/0.29	1.54/1.25/0.59	1.36/0.78/-0.80	1.76
3	0.34/0.19/-0.20	0.68/039/-0.40	-0.08/-0.66/-2.24	2.34
4	0.02/-0.165/-0.56	0.04/-0.33/-1.12	-1.86/-2.24/-3.02	4.19
5	-0.465/-0.56/-0.755	-0.93/-1.12/-1.51	-3.34/-3.92/-5.50	6.12
6	-0.835/-0.98/-1.375	-1.67/-1.96/-2.75	-5.16/-5.64/-7.32	10.58
7	-1.29/-1.41 /-1.83	-2.58/-2.82/-3.66	– / – / –	–

The results of the stepwise calculation demonstrate the quantitative contribution of each factor to the variation in compressive strength of the asphalt concrete specimen. Table III outlines the absolute and relative strength increments associated with changes in density (X_1), moisture content (X_2), and heating or cooling temperature (X_3).

TABLE III. STEPWISE CALCULATION RESULTS OF COMPRESSIVE STRENGTH VARIATION OF ASPHALT CONCRETE

Step-by-step change in road surface strength indicators, %			Σ
X_1	X_2	X_3	
3.08 (6.08 %)	2.50 (4.93 %)	1.18 (2.33 %)	6.76 (13.34 %)
1.36 (2.68 %)	0.78 (1.54 %)	0.80 (1.58 %)	2.94 (5.80 %)
0.08 (0.16 %)	0.66 (1.30 %)	2.24 (4.42 %)	2.98 (5.88 %)
1.86 (3.67 %)	2.24 (4.42 %)	3.02 (5.96 %)	7.12 (14.05 %)
3.34 (6.60 %)	3.92 (7.73 %)	5.50 (10.85 %)	12.76 (25.18 %)
5.16 (10.18 %)	5.64 (11.13 %)	7.32 (14.44 %)	18.12 (35.75 %)
14.88 (29.37 %)	15.74 (31.05 %)	20.06 (39.58 %)	50.68 (100 %)

The obtained values characterize the distribution of total strength variation among the considered parameters and indicate their relative influence under the studied temperature and moisture conditions. The step-by-step calculations reveal that asphalt concrete temperature (X_3) has the greatest impact on compressive strength variation among the investigated parameters. At step 6, the temperature's relative contribution reaches 35.75%. Meanwhile, the contribution of asphalt concrete density (X_1) does not exceed 0.16% when its values vary within the range of 0.99–0.87 t/m³. The influence of specimen moisture content (X_2), when the moisture content varies from 0% to 8%, ranges from 0.66% to 11.13%. This distribution of contributions requires further physical interpretation. The dominant contribution of temperature (X_3) at step 6 (35.75%) is consistent with the well-established rheological behavior of bituminous binders. Asphalt concrete is a viscoelastic composite whose mechanical response is primarily governed by the viscosity–temperature relationship of the bitumen phase. The bitumen grade used in this study (BND 90/130) has a standard softening point of approximately 43–45 °C using the Ring-and-Ball method (GOST 11506). As the specimen temperature approaches and exceeds this threshold, the binder transitions from an elastic-dominant response to a viscous-dominant response, leading to a significant reduction in compressive strength, and is commonly referred to as the temperature susceptibility of bitumen. Conversely, at −20 °C, the binder becomes brittle and stiff, resulting in higher compressive strength values. The temperature range of approximately 90 °C (-20 to +70 °C) spans both the brittle and softening regimes. This explains why temperature accounts for the largest share of strength variability. Authors in [15, 16] reported a three- to fivefold reduction in compressive strength across comparable temperature ranges. The negligible contribution of density ($X_1 \leq 0.16\%$) can be explained by the limited variation of density within the investigated range. The studied density interval (0.87–0.99 t/m³) corresponds to compaction coefficients of approximately 0.95–0.99 relative to the standard Proctor density, typical of well-compacted asphalt mixtures. Within this relatively narrow range, the compressive strength of asphalt concrete varies slightly because the internal friction and interlocking of aggregate particles remain nearly constant. Under these conditions, the dominant performance-controlling mechanism is rheological rather than packing-related; the viscosity, softening point, and temperature susceptibility of the bituminous binder greatly influence the strength response. Authors in [17] showed that mixture structure and stiffness are more sensitive to volumetric changes under low-compaction conditions. The interaction coefficient, B_{23}=-0.05, indicates a weak, yet physically meaningful, coupling between moisture content X_2 and temperature X_3. The negative sign suggests that, at elevated temperatures, a higher moisture content simultaneously present with temperature leads to a greater reduction in compressive strength than the one that would be expected from the independent effects of these factors. This behavior is consistent with the plasticizing action of water on bitumen films and moisture-induced debonding, which becomes more pronounced at higher temperatures. Although B_{23} is smaller in magnitude than the main effects (B_1= 1.95, B_2= 1.66, B_3= 0.87), its physical significance should not be overlooked. Under combined high-temperature and high-moisture conditions (during warm and wet periods), the interaction effect may accelerate strength degradation beyond predictions based on a single factor. Authors in [18] revealed that moisture-induced damage in asphalt concrete is strongly influenced by temperature and becomes more pronounced at elevated temperatures.

B. Result Interpretation

The results show that temperature effects (X3) and asphalt concrete moisture content (X2) have the most significant influence on the strength of road pavements. Therefore, during motorway operation, special attention should be paid to water accumulation conditions on pavement surfaces, particularly in areas where increased moisture can decrease the strength of the road surface, as depicted in Figure 3. The curve in Figure 4 shows the stepwise approximation of the desired point, whereas Figure 5 demonstrates the correlation between the compressive strength properties of asphalt concrete and the experimental and calculated values. The coefficient of determination between the predicted and experimental compressive strength values is R^2 = 0.8001, indicating a satisfactory level of agreement between the model and the experimental data.

IV. CONCLUSIONS

This study confirms that the compressive strength of asphalt concrete pavement is significantly affected by density, moisture content, and temperature. The analysis shows that maintaining a high compaction level is significant to preserving strength characteristics. In the conditions considered, the asphalt concrete compaction coefficient should be at least 0.99;

a density reduction to 0.87 t/m³ corresponds to a critical decrease in strength.

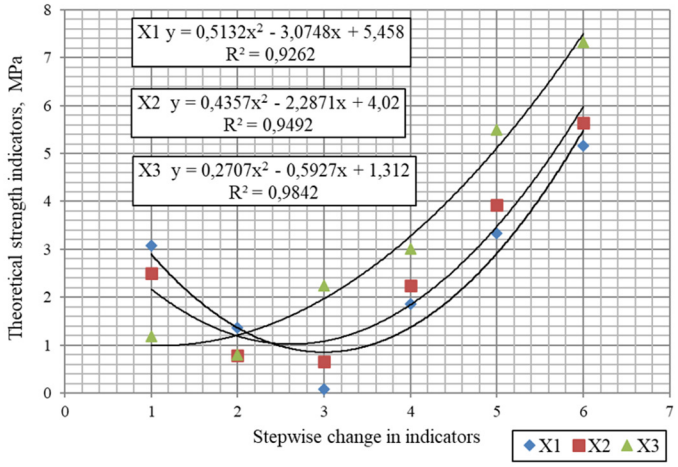

Fig. 3. Stepwise contribution of parameters to compressive strength variation.

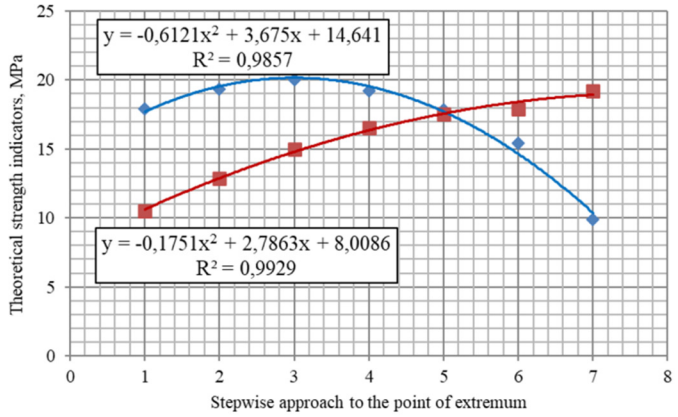

Fig. 4. The process of reducing the strength characteristics of asphalt concrete under compression on a hydraulic press.

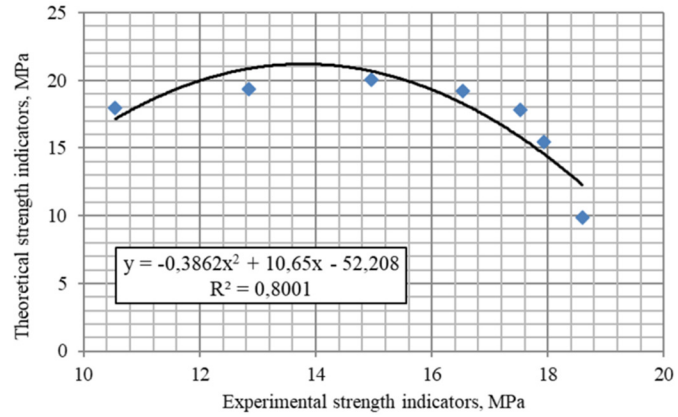

Fig. 5. Correlation between the compressive strength properties of asphalt concrete and experimental and calculated values.

Moisture content also plays an important role in strength degradation. Within the investigated range, increasing moisture content by up to 8% leads to a noticeable reduction in compressive strength, especially when combined with unfavorable temperature conditions. Temperature changes have the most pronounced influence on strength variation. The results demonstrate that temperature variation from −20 °C to +70 °C contributes substantially more to strength reduction than changes in density and moisture content. The proposed gradient-based calculation approach enables evaluation of compressive strength behavior under the combined influence of the examined factors. The model determines the minimum compressive strength corresponding to critical operating conditions and provides a quantitative assessment of the relative influence of density (X_1), moisture (X_2), and temperature (X_3). The results indicate that temperature and moisture are the dominant factors in the degradation of the strength of asphalt concrete pavements and should be considered in their design and operation.

DECLARATION OF COMPETING INTERESTS

The authors declare that they have no known competing financial interests or personal relationships that could have appeared to influence the work reported in this paper.

ACKNOWLEDGMENT

The authors are grateful to the L.B. Goncharov Kazakh Automobile and Road Institute for providing laboratory infrastructure and technical support during the experimental studies. This research received no external funding.

DATA AVAILABILITY

The data that support the findings of this study are available from the corresponding author upon reasonable request.

AI USE AND DECLARATION OF GENERATIVE AI USE

During the preparation of this work, the authors used Claude (Anthropic) to assist with language editing and improve the clarity of the manuscript text. After using this tool, the authors reviewed and edited the content as needed and took full responsibility for the content of the publication.

REFERENCES

[1] A. Tulebekova, A. Zhankina, R. Imambayeva, B. Makhiyev, A. Khapin, and D. Anop, "A practical solution for improving soil bases in problematic engineering conditions," *International Journal of GEOMATE*, vol. 25, no. 108, Aug. 2023, https://doi.org/10.21660/2023.108.3849.

[2] V. B. Nguyen, "Deterioration Analysis of Pavement Structures Incorporating Polymer-Modified Asphalt," *Engineering, Technology & Applied Science Research*, vol. 14, no. 6, pp. 18649–18654, Dec. 2024, https://doi.org/10.48084/etasr.9195.

[3] W. Dai, G. Li, X. Zhou, Y. Zhang, and J. Wang, "Research on void characteristics during compaction of asphalt mixtures," *Construction and Building Materials*, vol. 416, Feb. 2024, Art. no. 135069, https://doi.org/10.1016/j.conbuildmat.2024.135069.

[4] A. Vaitkus, L. Žalimienė, J. Židanavičiūtė, and D. Žilionienė, "Influence of temperature and moisture content on pavement bearing capacity with improved subgrade," *Materials*, vol. 12, no. 23, Nov. 2019, Art. no. 3826, https://doi.org/10.3390/ma12233826.

[5] *GOST 9128-2013 Asphaltic concrete and polymer asphaltic concrete mixtures, asphaltic concrete and polymer asphaltic concrete for roads and aerodromes. Specifications*. Moscow, Russia: Standartinform, 2013.

[6] S. Liu, J. Wang, Y. Li, and Z. Chen, "Enhancement of MICP-treated sandy soils against environmental deterioration," *Journal of Materials in*

Civil Engineering, vol. 31, no. 12, Dec. 2019, Art. no. 04019294, https://doi.org/10.1061/(ASCE)MT.1943-5533.0002959.

[7] W. A. Abd-Alkhaleq and M. Q. Ismael, "Enhancing the Moisture Resistance in Asphalt Mixtures Using Epoxy Resin," *Engineering, Technology & Applied Science Research*, vol. 15, no. 5, pp. 26868–26873, Oct. 2025, https://doi.org/10.48084/etasr.12476.

[8] Y. M. H. AlHamdo, A. H. K. Albayati, and M. J. Al-Kheetan, "High-temperature properties of hot mix asphalt modified with different nanomaterials," *Nanomaterials*, vol. 15, no. 24, Dec. 2025, Art. no 1845, https://doi.org/10.3390/nano15241845.

[9] M. K. Pshembayev, C. N. Kiyalbai, D. Y. Yessentay, and G. Tleulenova, "Regulation of the water-heat regime of the subgrade of cement-concrete road," *International Journal of GEOMATE*, vol. 25, no. 111, Nov. 2023, https://doi.org/10.21660/2023.111.4035.

[10] A. K. Kiyalbai, S. N. Kiyalbay, G. A. Espaeva, and N. Z. Madanbekov, *Theoretical and Experimental Methods of Transport Construction: Road Conditions and Fundamentals of Road Thermotechnics*. Almaty, Kazakhstan: Adal Kitap, 2023.

[11] Y. Gao, X. Tang, J. Chu, and J. He, "Microbially induced calcite precipitation for seepage control in sandy soil," *Geomicrobiology Journal*, vol. 36, no. 4, pp. 366–375, Apr. 2019, https://doi.org/10.1080/01490451.2018.1556750.

[12] [12] B. Jiang, S. Wu, F. Huang, F. Zhou, and X. Li, "Effect of microbially induced calcium carbonate precipitation on swelling and performance degradation of expansive soil," *Applied Sciences*, vol. 15, no. 12, Jun. 2025, Art. no. 6570, https://doi.org/10.3390/app15126570.

[13] S. R. Harnaeni, F. P. Pramesti, A. Budiarto, and A. Setyawan, "The effect of temperature changes on mechanistic performance of hot mix asphalt as wearing course with different gradation types," in *IOP Conference Series: Materials Science and Engineering*, vol. 403, 2018, Art. no. 030026, https://doi.org/10.1063/1.5042946.

[14] Haizhen, "A mathematical model of freezing process under Qinghai–Tibet Highway roadbed," 1999.

[15] G. Airey, "Rheological properties of styrene butadiene styrene polymer modified road bitumens," *Fuel*, vol. 82, no. 14, pp. 1709–1719, Oct. 2003, https://doi.org/10.1016/S0016-2361(03)00146-7.

[16] Y. Zhang, Y. Zhu, W. Wang, Z. Ning, S. Feng, and K. Höeg, "Compressive and tensile stress–strain-strength behavior of asphalt concrete at different temperatures and strain rates," *Construction and Building Materials*, vol. 311, Dec. 2021, Art. no. 125362, https://doi.org/10.1016/j.conbuildmat.2021.125362.

[17] A. A. A. Molenaar and N. Li, "Prediction of compressive and tensile strength of asphalt concrete," *International Journal of Pavement Research and Technology*, vol. 7, no. 5, pp. 368–374, 2014, https://doi.org/10.6135/ijprt.org.tw/2014.7(5).368.

[18] N. Kringos, T. Scarpas, C. Kasbergen, and P. Selvadurai, "Modelling of combined physical–mechanical moisture-induced damage in asphaltic mixes, Part 1: Governing processes and formulations," *International Journal of Pavement Engineering*, vol. 9, no. 2, pp. 115–128, Apr. 2008, https://doi.org/10.1080/10298430701792127.